

Synthesis and Photoluminescence of Lithium Aluminium Borate Phosphors

$\text{LiAlB}_2\text{O}_5:\text{Eu}^{3+}$

S. R. Khandekar¹, R. S. Palaspagar^{2#}

¹Department of Chemistry, Indira Mahavidyalaya, Kalamb, Maharashtra, India

²Department of Physics, Shivramji Moghe College, Kelapur (Pandharkawada), Maharashtra, India

Corresponding author E-mail: palaspagarritesh@gmail.com

ABSTRACT

The Lithium mixed Borates are good host materials for luminescent ions. The powder sample of the Eu^{3+} doped Lithium Alumino-Borate Phosphor $\text{LiAlB}_2\text{O}_5:\text{Eu}^{3+}$ has been prepared by solution Combustion method. The phase and structure of the as prepared material was confirmed by powder XRD technique. The photoluminescence properties of $\text{LiAlB}_2\text{O}_5:\text{Eu}^{3+}$ have been investigated. The phosphor $\text{LiAlB}_2\text{O}_5:\text{Eu}^{3+}$ exhibits strong absorption over a wide UV range from 300 – 500 nm. It can be seen clearly that the charge transfer transition from the O^{2-} to Eu^{3+} excitation line at 254 nm wavelengths is very stronger than the intraconfiguration $4f^6$ excitation lines (394 nm, 382 nm). The phosphor $\text{LiAlB}_2\text{O}_5:\text{Eu}^{3+}$ shows intense red emission 614 nm corresponds to $5D_0 \rightarrow 7F_2$ when excited by 254 nm radiation. The red emission could be excited by NUV radiation of 390 nm. The phosphor $\text{LiAlB}_2\text{O}_5:\text{Eu}^{3+}$ could be a potential red emitting component in lamps and display applications and also in solid state lighting.

Keywords : Borate, Red Phosphor, Combustion synthesis, Photoluminescence.

I. INTRODUCTION

In the past few years aluminum borates have attracted much research interest because of their potential applications as nonlinear optical materials [i-ii], low thermal expansive ceramics [iii], and luminescence hosts [iv-v]. The excellent nonlinear optical property of alkali borate crystals mainly comes from their anionic groups [vi]. According to the previous work [vii], the larger the distortions in oxygen polyhedra or any other anionic groups of a structure and the more inhomogeneous the electron density distribution on the bonds in these groups, the higher the values of the second-order microscopic susceptibility. The charge distribution on the conjugated n orbital of $[\text{B}_3\text{O}_7]^{5-}$ is

asymmetry, so this kind of anionic group has a great second order microscopic susceptibility. In order to enhance the second-order microscopic susceptibility, we hope to replace tetra-coordinate B of $[\text{B}_3\text{O}_7]^{5-}$ groups with other atoms. Al seems a good candidate since it is often tetrahedrally coordinated in compounds and has an outer electronic structure similar to B. Therefore, a new compound LiAlB_2O_5 is expected to exist if the tetra-coordinated B can be replaced by Al. The diffraction pattern of LiAlB_2O_5 is reported by He et al. [viii].

II. MATERIAL AND METHOD

The powder samples of $\text{LiAl}(1-x)\text{B}_2\text{O}_5:x\text{Eu}^{3+}$ ($x = 0.005, 0.01, 0.03, 0.05, \text{ and } 0.07$) were prepared by a

solution combustion technique which is described earlier [ix-xii]. The stoichiometric amounts of high purity starting materials, $\text{Li}(\text{NO}_3)_2$ (A.R.), $\text{Al}(\text{NO}_3)_3 \cdot 9\text{H}_2\text{O}$ (A.R.), Eu_2O_3 (high purity 99.9%), H_3BO_3 (A.R.), $\text{CO}(\text{NH}_2)_2$ (A.R.) have been used for phosphor preparation. The stoichiometric amounts of the ingredients were thoroughly mixed in an agate mortar, adding little amount of de-ionized water to obtain an aqueous homogeneous solution. The aqueous solution was then transferred into a china basin and slowly heated at lower temperature of 70°C in order to remove the excess water. The solution was then introduced into a preheated muffle furnace maintained at 550°C . The solution boils foams and ignites to burn with flame; a voluminous, foamy powder was obtained. The entire combustion process was over in about 5 min. Following the combustion, the resulting fine powders were annealed in a carbon reducing atmosphere at temperature 850°C for 90 min. and suddenly cooled to room temperature. The prepared materials were characterized by powder XRD and FE-SEM. Powder X-ray diffraction measurements were taken on Rigaku Miniflex II X-ray Diffractometer and compared with the ICDD files. Surface morphology of the calcined particles was observed by scanning electron microscopy (FE-SEM). PL & PLE measurements at room temperature were performed on Hitachi F-7000 spectrofluorometer with spectral resolution of 2.5 nm.

III. RESULTS AND DISCUSSION

3.1 X-ray Diffraction Pattern

The XRD pattern of the host lattice of LiAlB_2O_5 shown in Fig. 1 found to be in good agreement with the standard ICDD file No. 01-070-5423. The compound LiAlB_2O_5 can be characterized as networks formed by $[\text{B}_2\text{AlO}_7]^{5-}$ rings and the structural units connect with each other. Every $[\text{B}_2\text{AlO}_7]^{5-}$ ring connects with four adjacent rings via bridging-oxygen atoms. Al has been introduced successfully into benzene-ring-like $[\text{B}_3\text{O}_7]^{5-}$ groups, but the properties of the Al atom are much different from those of B. The bond length of Al-

O is more than 1.7 \AA while that of B-O is less than 1.5 \AA , so the distribution of electron density on the $[\text{B}_2\text{AlO}_7]^{5-}$ ring will be more inhomogeneous.

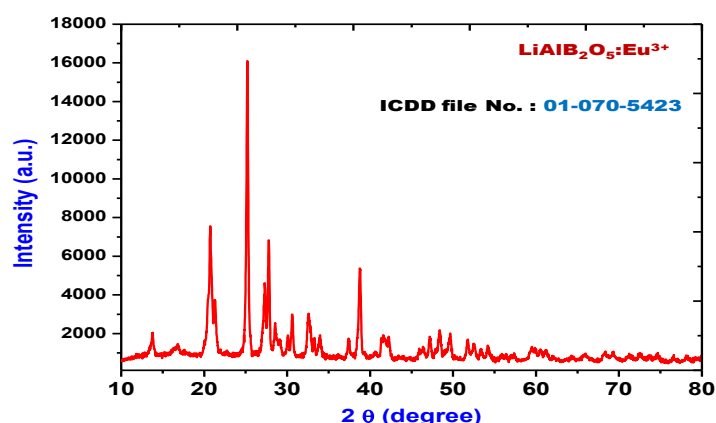


FIG. 1 XRD PATTERN OF $\text{LiAl}(0.95)\text{B}_2\text{O}_5:0.05\text{Eu}^{3+}$ PHOSPHOR.

3.2 FE-SEM micrographs of phosphor powders

FE-SEM Image of $\text{LiAl}(1-x)\text{B}_2\text{O}_5:\text{Eu}^{3+}$ is shown in Fig. . FE-SEM study was carried out to investigate the surface morphology of the phosphor. The first time investigation on the morphology of $\text{LiAl}(1-x)\text{B}_2\text{O}_5$ phosphor was reported in this work as morphology of the phosphor is not reported till date which has spherical like structure. The particles possess foamy like morphology formed from highly agglomerated crystallites.

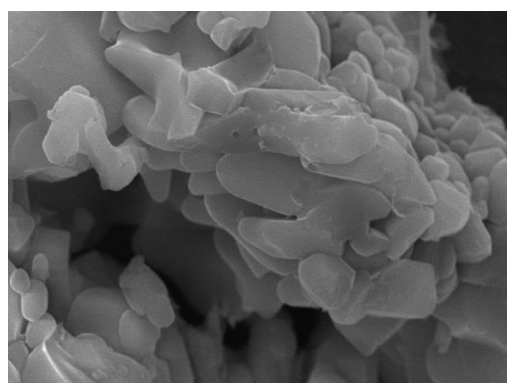


FIG. 2 FE-SEM MICROGRAPH OF $\text{LiAl}(0.95)\text{B}_2\text{O}_5:0.05\text{Eu}^{3+}$ PHOSPHOR.

3.3 Photoluminescence analysis of $\text{LiAl}_2\text{B}_2\text{O}_5:\text{Eu}^{3+}$

The excitation and emission spectra of $\text{LiAl}(1-x)\text{B}_2\text{O}_5:x\text{Eu}^{3+}$ ($\text{LABO}:\text{Eu}$) ($x=0.005, 0.01, 0.03, 0.05,$ and 0.07) phosphors at $\lambda_{\text{em}} = 614 \text{ nm}$ is shown in Fig. . The excitation spectrum of $\text{LABO}:\text{Eu}$ contains an intense broad band in the wavelength range $200\text{--}300 \text{ nm}$ with a maximum at 254 nm and a group of peaks in the longer wavelength region. The former is due to the charge transfer band (CTB) of $\text{Eu}^{3+} \rightarrow \text{O}^{2-}$ and the latter f-f transitions within $\text{Eu}^{3+} 4f_6$ configuration. The excitation spectra consist of sharp f-f transition lines in the wavelength range 300 nm to 500 nm , including $7F_0 \rightarrow 5H_3$ (319 nm), $7F_0 \rightarrow 5D_4$ (362 nm), $7F_0 \rightarrow 5L_7$ (382 nm), $7F_0 \rightarrow 5L_6$ (394 nm , stronger), and $7F_0 \rightarrow 5D_3$ (415 nm). It can be seen clearly that the charge transfer transition from the O^{2-} to Eu^{3+} excitation line at 254 nm wavelengths is very stronger than the intraconfiguration $4f_6$ excitation lines (394 nm , 382 nm). The emission spectra of $\text{LABO}:\text{Eu}$ under 254 nm excitation with different Eu contents shows several emission lines peaking at $579, 592, 614,$ and 655 nm . The most intense emission peak is observed at 614 nm due to $5D_0 \rightarrow 7F_2$ electric dipole transition, and the other emission peaks are ascribed to $5D_0 \rightarrow 7F_1$ and $5D_0 \rightarrow 7F_4$ magnetic dipole transition of Eu^{3+} , respectively. The result indicates that most of the Eu^{3+} is located at sites without inversion symmetry. Fig. shows the effect of Eu-doped concentration on the emission (at 614 nm) intensity of $\text{LABO}:\text{Eu}$ phosphors for 254 nm excitation. It indicates that the emission intensity increases with increasing Eu^{3+} concentration from $x=0.005$ to $x=0.05$. The most intense peak is observed at a concentration of $x=0.05$, and then the intensity decreases, this is due to the facts that the substitution of Eu^{3+} for Al^{3+} increases and that the CTB wavelength increases with the concentration increasing of Eu^{3+} ions. The most prominent emission peak is observed at 614 nm which can be assigned to $5D_0 \rightarrow 7F_2$ transition.

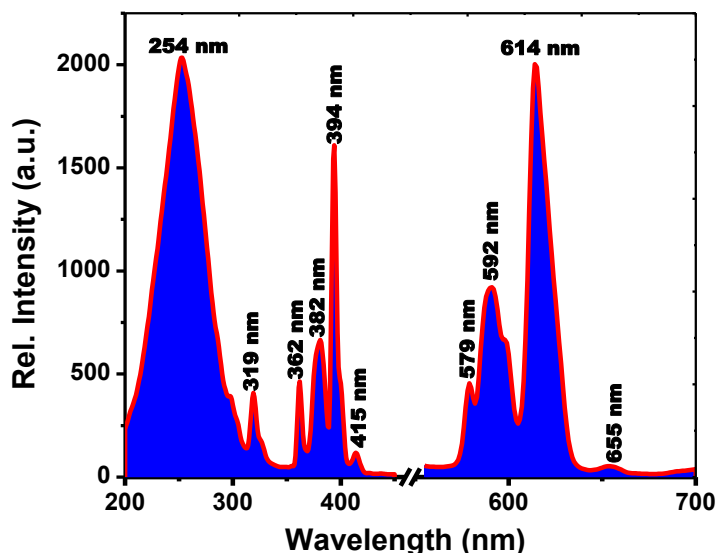


Fig. 3 The excitation and emission spectra of $\text{LiAl}(0.95)\text{B}_2\text{O}_5:0.05\text{Eu}^{3+}$ phosphors. ($\lambda_{\text{ex}} = 254 \text{ nm}$, and $\lambda_{\text{em}} = 614 \text{ nm}$).

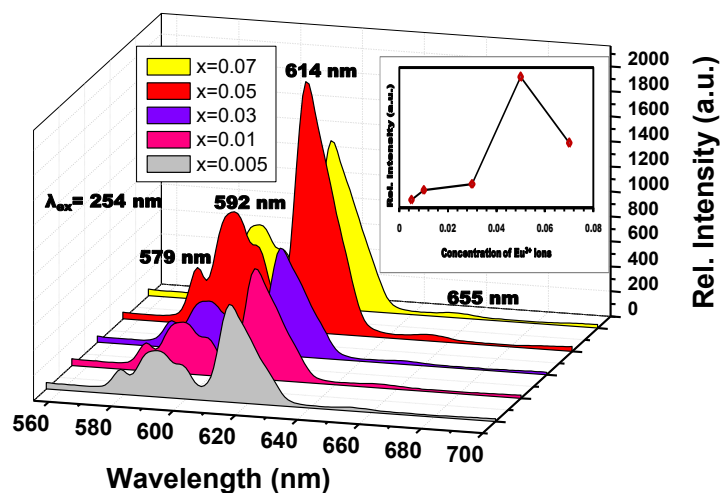


Fig. 4 The emission spectra of $\text{LiAl}(1-x)\text{B}_2\text{O}_5:x\text{Eu}^{3+}$, with x equal to $0.005, 0.01, 0.03, 0.05,$ and $0.07,$ respectively.

The CIE chromaticity coordinates for $\text{LiAl}(0.95)\text{B}_2\text{O}_5:0.05\text{Eu}^{3+}$ were calculated from the PL spectra under 254 nm excitation and marked with a white star in the CIE 1931 chromaticity diagram in Fig. . The chromaticity coordinates (x, y) of this phosphor are calculated to be $(0.67, 0.32)$, respectively, which indicates that the emission color of the $\text{LiAl}(0.95)\text{B}_2\text{O}_5:0.05\text{Eu}^{3+}$ phosphors is located in the reddish-orange region.

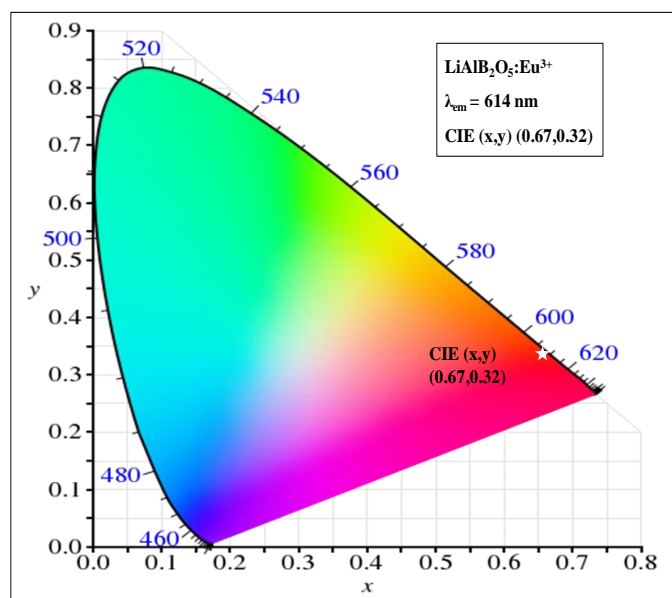


Fig. 5 Chromaticity coordinates of $\text{LiAl(0.95)B}_2\text{O}_5:0.05\text{Eu}^{3+}$ phosphor in the CIE 1931 chromaticity diagram.

IV. CONCLUSION

The phosphor $\text{LiAlB}_2\text{O}_5:\text{Eu}^{3+}$ can be synthesized by a simple, time saving and cost effective solution combustion technique. The excitation spectra show that the intraconfiguration $4f^6$ excitation lines are weaker than the charge transfer transition from O^{2-} to Eu^{3+} . The PL spectra show the strongest emission at 614 nm corresponding to the electric dipole $5D_0 \rightarrow 7F_2$ transition of Eu^{3+} in LiAlB_2O_5 due to the non-centrosymmetric nature of the Eu^{3+} site, which results in pure red color emission. The phosphor possesses excellent red emitting property which can be attractive to a wide range of potential applications.

V. ACKNOWLEDGEMENT

Authors are thankful to the Chairman of FIST-DST project SGB Amravati University Amravati, for providing XRD facility to this work.

REFERENCES

- N. Ye, W. R. Zeng, B. C. Wu, X. Y. Huang, C. T. Chen, Z. Kristallogr., New Cryst. Struct., 213 (1998) 452.
- [ii] N. Ye, W. R. Zeng, J. Jiang, B. C. Wu, C. T. Chen, B. H. Feng, X. L. Zhang, J. Opt. Soc. Am. B, 17 (2000) 764.
- [iii] J. F. MacDowell, J. Am. Ceram. Soc., 73 (1990) 2287.
- [iv] F. Lucas, S. Jaulmes, M. Quarton, T. Le Mercier, F. Guillen, C. Fouassier, J. Solid State Chem., 150 (2000) 404.
- [v] H. You, G. Hong, Mater. Res. Bull., 32 (1997) 78.
- [vi] W. D. Cheng, J. X. Lu, Chin. Sci. Bull., 42 (1997) 606.
- [vii] S. F. Radaev, B. A. Maximov, V. I. Simonov, B. V. Andreev, V. A. D'yakov, Acta Crystallogr. B, 48 (1992) 154.

-
- [viii] M. He, X. L. Chen, Y. C. Lan, H. Li, and Y. P. Xu, *J. Solid State Chem.*, 156 (2001) 181.
- [ix] R. S. Palaspagar, R. P. Sonekar, S. K. Omanwar, *AIP Conf.Proc.* 1536 (2013) 895-897.
- [x] A.B. Gawande, R.P. Sonekar, S.K. Omanwar, *J. Lumin.* 149 (2014) 200-203.
- [xi] R. S. Palaspagar, R. P. Sonekar, S. K. Omanwar, *IOSR J. App. Phy. Special issue* (2014) 11-14.
- [xii] R. J. Xie, N. Hirosaki, *Sci. Technol. Adv. Mater.*, 8 (2007) 588.